

Ultrafast response of nonlinear refractive index of silver nanocrystals embedded in glass

Y. Hamanaka^{a)} and A. Nakamura

Center for Integrated Research in Science and Engineering and Department of Crystalline Materials Science, Graduate School of Engineering, Nagoya University, Nagoya 464-8603, Japan

S. Omi

Materials Research Laboratory, HOYA Corporation, Akishima, Tokyo 196-0021, Japan

N. Del Fatti, F. Vallée, and C. Flytzanis

Laboratoire d'Optique Quantique du CNRS, Ecole Polytechnique, 91128 Palaiseau cedex, France

(Received 19 April 1999; accepted for publication 27 July 1999)

Ultrafast Kerr-type nonlinearities and relaxation dynamics of photoexcited electrons in silver nanocrystals embedded in glass have been investigated by means of femtosecond pump and probe spectroscopy. The transient absorption spectrum induced by the surface plasmon excitation shows a redshift and broadening of the surface plasmon band. The additional broadening is ascribed to the increase of surface plasmon damping and the redshift originates from a change in the real part of the dielectric function of the silver nanocrystals due to nonequilibrium electron heating. The observed redshift yields the nonlinear refractive index n_2 of $+2.4 \times 10^{-10}$ esu and its time response is 1.9 ps.

© 1999 American Institute of Physics. [S0003-6951(99)01938-5]

Metal nanocrystal–glass composites have attracted much attention from the point of view of nonlinear optics for their large nonlinear susceptibilities and fast response time.^{1–3} The response time of copper nanocrystals is as short as 0.7 ps in the weak excitation limit,³ and such an ultrafast nonlinear response is interpreted in terms of generation and relaxation of hot electrons. Third-order susceptibilities $\chi^{(3)}$ in noble metal nanocrystal–glass composites are enhanced to the order of 10^{-7} esu around the surface plasmon (SP) resonance frequency.^{1,2} The enhancement of nonlinearities of the composite results from a dielectric confinement effect.^{1,2,4} A Kerr-type nonlinearity has also been investigated for copper nanocrystal system.⁵

The SP dynamics in metal nanocrystals in the femtosecond time region has been studied by several groups.^{3,6–9} The large broadening of the SP band has been observed for gold, silver, and copper nanocrystals under the femtosecond pulse excitation. As the interband transition of the d band to sp bands lies in the same spectral region as the SP resonance in gold and copper system, both the conduction electrons and the SPs contribute to the nonlinear response around the SP resonance.⁴ In silver, on the other hand, the SP resonance is far from the interband transition.⁴ Thus, we can separately investigate both contributions to the dynamical properties of the nonlinear response. In this letter, we report on the femtosecond nonlinear optical response due to SPs in a silver nanocrystal–glass composite and a nonlinear refractive index n_2 of silver nanocrystals with a radius of 3 nm.

Silver nanocrystals embedded in BaO–P₂O₅ glass were prepared by means of conventional melt and heat-treatment procedures.² The mean crystallite radius and the standard deviation of the mean radius were 3 and 0.3 nm, respectively. The volume fraction of the silver nanocrystals and the nanocrystal concentration were 3×10^{-4} and 5×10^{15}

cm⁻³, respectively. The sample thickness was 12 μ m. The metal nanocrystal embedded in glass can be regarded as an elastic sphere in which SP modes and mechanical radial modes are excited. The interface property is not affected by the matrix composition. For the sample used in this study, we have observed the oscillatory behavior of the transient transmission due to coherent excitation of the breathing mode of the silver nanocrystals,¹⁰ which indicates the clear interface between the nanocrystal and the glass. Transient absorption spectra were measured by a pump and probe method using an amplified Ti:sapphire laser operating at 10 Hz. The pulse duration, photon energy, and pulse energy are 300 fs, 1.6 eV, and 1 mJ, respectively. Output pulses were frequency doubled (3.2 eV) by a 1-mm-thick KDP crystal and used as a pump pulse. The pulse duration of the pump pulse was 500 fs. The fundamental pulse was focused onto a 1 cm cell containing H₂O to generate a white-light continuum probe pulse by self-phase modulation.

The absorption spectrum of silver nanocrystals embedded in glass is shown in Fig. 1(a). A broad SP band is observed at 3.0 eV, and absorption due to interband transitions (≥ 3.9 eV) is not seen in this photon energy range. Figure 1(b) shows differential absorption spectra around the SP band after excitation with a photon energy of 3.2 eV. We observe a decrease of absorption at the peak and an increase of absorption at the low-energy side of the peak. The asymmetric feature of the differential spectrum suggests both the redshift and broadening of the SP band after pulse excitation. To investigate the time-dependent behaviors of the spectrum, we analyzed the observed spectra using a spectral fitting method.⁸ The line shape of the SP band can be approximately fitted to a Lorentz function for small nanocrystals where only the lowest-order absorption is dominant.⁴ We suppose as a line shape of the SP band a Lorentz function convoluted with a modified Gauss function which expresses the inhomogeneous broadening due to the inhomogeneity in

^{a)}Electronic mail: hamanaka@cirse.nagoya-u.ac.jp

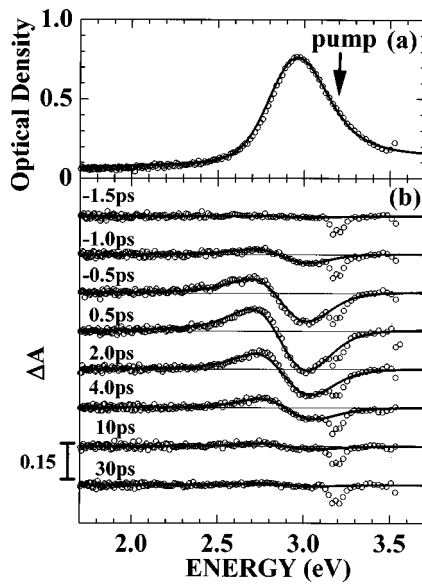


FIG. 1. (a) Absorption spectrum of silver nanocrystals with a radius of 3 nm embedded in glass. The arrow indicates the pump photon energy. (b) Differential absorption spectra ΔA for various delay times. The small dip at 3.2 eV is due to the scattered light of the pump pulse. Solid curves represent fitted curves.

the size and shape of the nanocrystals. The best-fitted spectrum for the linear absorption spectrum is shown in Fig. 1(a) by the solid curve. The full width at half maximum (FWHM) of the Lorentz component is 280 meV. Taking an additional broadening of Lorentz function ΔW , a peak shift ΔP , and a change in absorption area ΔS of the SP band as adjustable fitting parameters, the differential spectra for various delay times are well reproduced by the solid curves as shown in Fig. 1(b). The fitted parameters of ΔW and ΔP are plotted as a function of delay times in Figs. 2(a) and 2(b). ΔW and ΔP depend on the excitation laser fluences: the redshift increases from 14 to 52 meV, when we increase the laser fluence from

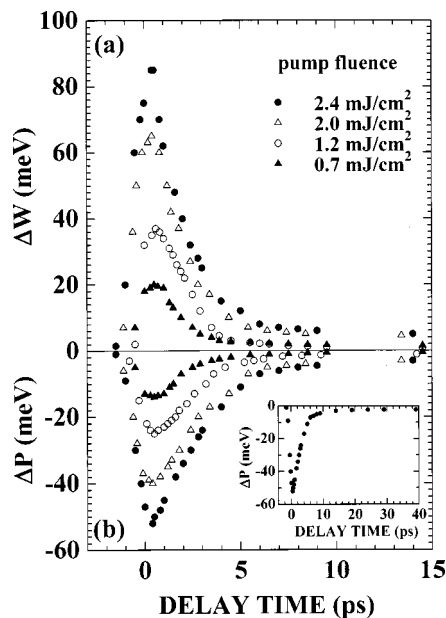


FIG. 2. Time evolutions of the additional broadening (a) and peak shift (b) of the SP band for the excitation photon fluences of 2.4, 2.0, 1.2, and 0.7 mJ/cm². The inset shows the decay behavior in the long delay time region for the fluence of 2.4 mJ/cm².

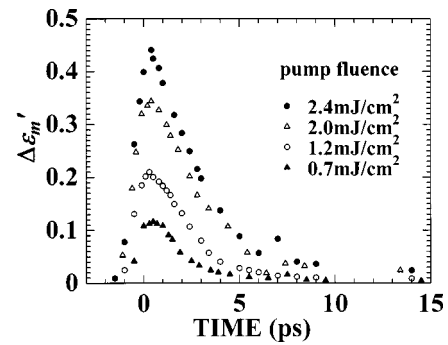


FIG. 3. Time evolutions of the change in the real part of the dielectric constant.

0.7 to 2.4 mJ/cm². Such a large redshift is in contrast to the result observed for gold nanocrystals in which the blueshift is initially observed and subsequently turns into a small redshift.⁷ ΔP decays to about 10% of the maximum value within 5 ps after the excitation, and the slow component lasts even after 40 ps [the inset of Fig. 2(b)]. The decay times of the fast component are analyzed from the decay curves assuming a two-component exponential decay, and they are 3.3, 3.0, 2.9, and 2.0 ps for the excitation laser fluences of 2.4, 2.0, 1.2, and 0.7 mJ/cm², respectively. The decay dynamics of ΔW [Fig. 2(a)] exhibit similar behavior. As the broadening of the SP band is caused by electron damping, the additional broadening indicates electron heating by excitation of SPs.^{3,7,8}

We now analyze the observed redshift taking into account a nonlinear dielectric function of the silver nanocrystals within the framework of the SP model for metal nanocrystals in a dielectric medium. SP resonance occurs at the frequency ω_s , for which the following relation is satisfied:⁴

$$[\epsilon'_m(\omega) + 2\epsilon_d(\omega)]^2 + [\epsilon''_m(\omega)]^2 = \text{minimum}, \quad (1)$$

where $\epsilon'_m(\omega)$ and $\epsilon''_m(\omega)$ are the real and imaginary parts of the metal dielectric function and $\epsilon_d(\omega)$ is a dielectric function of glass. Assuming that $\epsilon'_m(\omega)$ and $\epsilon''_m(\omega)$ are changed but $\epsilon_d(\omega)$ remains constant ($=1.75$) by the femtosecond pulse pumping, the changes in $\epsilon'_m(\omega)$ and $\epsilon''_m(\omega)$ give rise to a resonance frequency shift. The above assumption is reasonable in our experiments because the pump photon energy is away below the absorption edge of the glass. The change $\Delta\epsilon''_m(\omega)$ of $\epsilon''_m(\omega)$ is related to the change $\Delta\gamma$ of the peak height γ by the following equation:⁴

$$\Delta\epsilon''_m/\epsilon''_m = -\Delta\gamma/\gamma. \quad (2)$$

The ratio $\Delta\gamma/\gamma$ at each delay time can be obtained from the spectral fitting analysis of the SP band. $\epsilon''_m(\omega)$ of silver nanocrystals strongly depends on the crystallite size, while the value of $\epsilon'_m(\omega)$ is almost the same as that of bulk silver.^{4,11} We estimated a $\epsilon''_m(\omega)$ value of 1.4 for the average radius of 3 nm from the measured data.⁴ Using Eqs. (1) and (2) and the measured data, we calculated $\Delta\epsilon'_m$ values. The obtained values are plotted as a function of delay time in Fig. 3. The maximum redshift of 52 meV for the excitation fluence of 2.4 mJ/cm² yields $\Delta\epsilon'_m(\omega) = +0.44$; $\epsilon'_m(\omega)$ changes from -6.29 to -5.85 . The time evolution of $\Delta\epsilon'_m(\omega)$ exhibits a two-component decay being similar to the decay behaviors of the redshift and broadening. Defining the decay time

as the time interval at which $\Delta\epsilon'_m(\omega)$ decreases to $1/e$ of the maximum value, the decay times are estimated to be 3.5, 3.3, 2.8, and 1.9 ps for excitation fluences of 2.4, 2.0, 1.2, and 0.7 mJ/cm², respectively. The change in the real part of the dielectric function by optical pulses is nothing but a nonlinear refractive index associated with the third-order polarization. The silver nanocrystal–glass composite shows plasmon-mediated Kerr-type nonlinearity with response time on a picosecond time scale. The optical nonlinearity of the matrix glass does not contribute to the observed nonlinearity because the $\chi^{(3)}$ value of the matrix glass is three orders of magnitude smaller than that of the silver nanocrystal–glass composite.

We now estimate values of $\chi_m^{(3)}$ and n_2 of the silver nanocrystals using the obtained value of $\Delta\epsilon'_m(\omega)$. The local electric field inside the nanocrystal E_i , which differs from the applied optical field E_0 , is written as

$$E_i = \frac{3\epsilon_d}{\epsilon_m + 2\epsilon_d} E_0 = f_i E_0, \quad (3)$$

where f_i is the local field factor.¹ $\Delta\epsilon'_m$ is related to $\text{Re } \chi_m^{(3)}$ as

$$\Delta\epsilon'_m = 3\pi \text{Re } \chi_m^{(3)} |E_i|^2. \quad (4)$$

Using the f_i value of 6.674 for the sample used in this study,² $\text{Re } \chi_m^{(3)}$ is estimated as $+1.1 \times 10^{-11}$ esu. The obtained value of $\text{Re } \chi_m^{(3)}$ gives the n_2 value of $+2.4 \times 10^{-10}$ esu. We note that the $\text{Re } \chi_m^{(3)}$ value is smaller than the absolute value of $\chi_m^{(3)}$ measured at the resonance peak by degenerate four-wave mixing (DFWM) using a nanosecond pulse laser [$|\chi_m^{(3)}| = 2.94 \times 10^{-9}$ esu (Ref. 2)], although we cannot directly compare $\text{Re } \chi_m^{(3)}$ with $|\chi_m^{(3)}|$. As was discussed in Ref. 12, the diffraction efficiency measured by DFWM depends on the laser pulse duration used in the measurement, when the nonlinear response time T_1 is longer than the pulse duration t_p . In this case, the nonlinear susceptibility is derived from the diffraction efficiency by considering the ratio of T_1 to t_p , T_1/t_p . If we do not correct for this factor, the measurement with a pulse longer than T_1 yields always values larger than the short pulse measurement. As the pulse duration used in this study (500 fs) is shorter than the fast (≈ 3 ps) and slow (≥ 40 ps) relaxation times, the susceptibility measured by the femtosecond pulse may be smaller by the factor t_p/T_1 than the nanosecond laser case.

In what follows, we discuss the decay behaviors of $\Delta\epsilon'_m$ and ΔW , which reflect an increase of electron damping by the plasmon excitation, using an electron–phonon coupling model.¹³ In this model, the cooling process of hot electrons is ascribed to the temperature equilibrium process between the electron and lattice systems via an electron–phonon interaction. In bulk metal crystals, the increase of the damping after femtosecond pulse excitation is mainly due to an increase in the electron–electron collision rate which depends on the square of the electron temperature (T_e^2).¹⁴ In metal nanocrystals, however, electron–nanocrystal surface collision also plays a role in the damping, when the crystallite size is small. The electron–nanocrystal surface collision rate is approximately proportional to the square of the electron temperature,¹⁵ which is similar to the electron–electron collision rate. Assuming that ΔW is proportional to T_e^2 , we cal-

culated time evolutions of T_e by using coupled differential equations for electron and lattice temperatures.¹³ The highest value of T_e in this study was obtained as 2750 K for the pump fluence of 2.4 mJ/cm². Defining the decay time of T_e in the same way as in the case of $\Delta\epsilon'_m$, the decay times are 4.0, 3.6, 3.0, and 2.6 ps for the pump fluences of 2.4, 2.0, 1.2, and 0.7 mJ/cm², respectively. The decay times of T_e and their dependence on pump fluences are almost in agreement with those of $\Delta\epsilon'_m$. Therefore, we attribute the change in the dielectric function to the generation of nonequilibrium hot electrons. The decay behavior reflects the cooling dynamics of hot electrons, but a slight discrepancy between the decay times of T_e and $\Delta\epsilon'_m$ indicates that $\Delta\epsilon'_m$ is not exactly proportional to T_e .

In summary, we have measured time evolutions of the SP resonance band in silver nanocrystals embedded in glass by femtosecond pump and probe spectroscopy. The SP band is broadened substantially after the excitation by femtosecond optical pulses, and shows the redshift. The additional broadening reflects the increase of the electron damping which is mainly determined by the collision with electrons and nanocrystal surfaces. The time evolution of the broadening on the picosecond time scale is interpreted in terms of the hot electron cooling within the electron–phonon coupling model. The redshift is attributed to the increase in the real dielectric constant of silver nanocrystals by the femtosecond optical pulse. The measured redshift yields the $\text{Re } \chi_m^{(3)}$ value of $+1.1 \times 10^{-11}$ esu and the n_2 value of $+2.4 \times 10^{-10}$ esu. The response time of n_2 is 1.9–3.5 ps depending on the laser fluence.

The present work was supported by a Grant-in-Aid for Scientific Research, and International Scientific Research (Joint Research) from the Ministry of Education, Science, Sports, and Culture of Japan and New Energy and Industrial Technology Development Organization (NEDO).

¹F. Hache, D. Ricard, C. Flytzanis, and U. Kreibig, *Appl. Phys. A: Solids Surf.* **47**, 347 (1988).

²K. Uchida, S. Kaneko, S. Omi, C. Hata, H. Tanji, A. Asahara, A. J. Ikushima, T. Tokizaki, and A. Nakamura, *J. Opt. Soc. Am. B* **11**, 1236 (1994).

³T. Tokizaki, A. Nakamura, S. Kaneko, K. Uchida, S. Omi, H. Tanji, and Y. Asahara, *Appl. Phys. Lett.* **65**, 941 (1994).

⁴U. Kreibig and M. Vollmer, *Optical Properties of Metal Clusters* (Springer, Berlin, 1995).

⁵R. F. Haglund, Jr., L. Yang, R. H. Magruder III, J. E. Wittig, K. Becker, and R. A. Zuhr, *Opt. Lett.* **18**, 373 (1993).

⁶J.-Y. Bigot, J.-C. Merle, O. Cregut, and A. Daunois, *Phys. Rev. Lett.* **75**, 4702 (1995).

⁷M. Perner, P. Bost, U. Lemmer, G. von Plessen, J. Feldmann, U. Becker, M. Mennig, M. Schmitt, and H. Schmidt, *Phys. Rev. Lett.* **78**, 2192 (1997).

⁸Y. Hamanaka, N. Hayashi, A. Nakamura, and S. Ohmi, *J. Lumin.* **76&77**, 221 (1998).

⁹H. Inouye, K. Tanaka, I. Tanahashi, and K. Hirao, *Phys. Rev. B* **57**, 11334 (1998).

¹⁰N. Del Fatti, C. Voisin, F. Chevy, F. Vallée, and C. Flytzanis, *J. Chem. Phys.* **110**, 11484 (1999).

¹¹P. B. Johnson and R. W. Christy, *Phys. Rev. B* **6**, 4370 (1972).

¹²Y. Li, M. Takata, and A. Nakamura, *Phys. Rev. B* **57**, 9193 (1998).

¹³S. I. Anisimov, B. L. Kapeliovich, and T. L. Perel'man, *Zh. Eksp. Teor. Fiz.* **66**, 776 (1974) [*Sov. Phys. JETP* **39**, 375 (1974)].

¹⁴R. N. Gurzhi, *Zh. Eksp. Teor. Fiz.* **35**, 965 (1959) [*Sov. Phys. JETP* **35**, 673 (1959)].

¹⁵N. Del Fatti, F. Vallée, C. Flytzanis, Y. Hamanaka, and A. Nakamura, *Chem. Phys.* (to be published).